Giant conductance oscillations in mesoscopic Andreev interferometers

1996 J. Phys.: Condens. Matter 8 L377

(http://iopscience.iop.org/0953-8984/8/26/001)

J. Phys.: Condens. Matter **8** (1996) L377–L384. Printed in the UK

LETTER TO THE EDITOR

Giant conductance oscillations in mesoscopic Andreev interferometers

N K Allsopp†, J Sánchez Cañizares‡, R Raimondi† and C J Lambert†

† School of Physics and Materials, University of Lancaster, Lancaster LA1 4YB, UK

‡ Departamento de Física de la Materia Condensada, C-XII, Universidad Autónoma de Madrid, E-28049, Madrid, Spain

Received 29 January 1996

Abstract. We analyse the electrical conductance $G(\phi)$ of a two-dimensional, phase-coherent structure in contact with two superconductors, which is known to be an oscillatory function of the phase difference ϕ between the superconductors. It is predicted that for a ballistic sample, the amplitude of oscillation will be enhanced by placing a normal barrier at the normal–superconducting interface, and that by tuning the strength of the barrier, it can be made orders of magnitude greater than values observed in recent experiments. Giant oscillations can also be obtained without a barrier, provided that a crucial sum rule is broken. This can be achieved by disorder-induced normal scattering. In the absence of zero-phase inter-channel scattering, the conductance possesses a zero-phase minimum and a maximum at $\phi = \pi$.

Andreev interferometers are a recently discovered paradigm of phase-coherent transport in mesoscopic superconducting structures. When a quasi-particle Andreev reflects from a normal–superconducting (N–S) interface, the phase of the outgoing excitation is shifted by the phase of the superconducting order parameter [1]. Consequently if a phase-coherent normal conductor is in contact with two superconductors with order parameter phases ϕ_1, ϕ_2, transport properties will be oscillatory functions of the phase difference $\phi = \phi_1 - \phi_2$. Several realizations of such Andreev interferometers are now available in the laboratory and for those in which disorder plays a dominant role [2–6], currently available theories [7–14] can be used to describe the observed generic features. In contrast, for systems such as a clean two-dimensional electron gas, smaller than the elastic mean free path [15], there is currently no quantitative theory which accounts for the intrinsic two-dimensional nature of such structures.

The aim of this letter is to develop a description of the clean limit which is capable of addressing questions such as those of the nature of the zero-phase extremum in $G(\phi)$ and the amplitude of oscillation. In some experiments [3, 4, 6] the amplitude is found to be several orders of magnitude smaller than $2e^2/h$, but in others [2, 5] it is a few multiples of $2e^2/h$. In what follows we predict that certain structures are capable of giant oscillations, with amplitudes many orders of magnitude greater than $2e^2/h$. Remarkably, the amplitude vanishes for very clean samples, and so to obtain a large effect, a degree of normal scattering must be introduced, in order that an approximate sum rule is broken. This occurs, for example, when a Schottky barrier is present at a clean N–S interface.

For simplicity we consider the zero-temperature limit, where the electrical conductance between two normal reservoirs can be written [9, 16] (in units of $2e^2/h$) as

$$G = T_0 + T_a + \frac{2(R_a R'_a - T_a T'_a)}{R_a + R'_a + T_a + T'_a}. \tag{1}$$

0953-8984/96/260377+08$19.50

In this expression, R_0, T_0 (R_a, T_a) are the coefficients for normal (Andreev) reflection and transmission for zero-energy quasi-particles from reservoir 1, while R_0', T_0' (R_a', T_a') are the corresponding coefficients for quasi-particles from reservoir 2. If each of the external leads connecting the reservoirs to the scatterer contains N open channels, these satisfy $R_0 + T_0 + R_a + T_a = R_0' + T_0' + R_a' + T_a' = N$ and $T_0 + T_a = T_0' + T_a'$. Furthermore, in the absence of a magnetic field, all reflection coefficients are even functions of ϕ, while the transmission coefficients satisfy $T_0'(\phi) = T_0(-\phi)$, $T_a'(\phi) = T_a(-\phi)$. Consequently on quite general grounds, in the absence of a field, G is predicted to be an even function of ϕ.

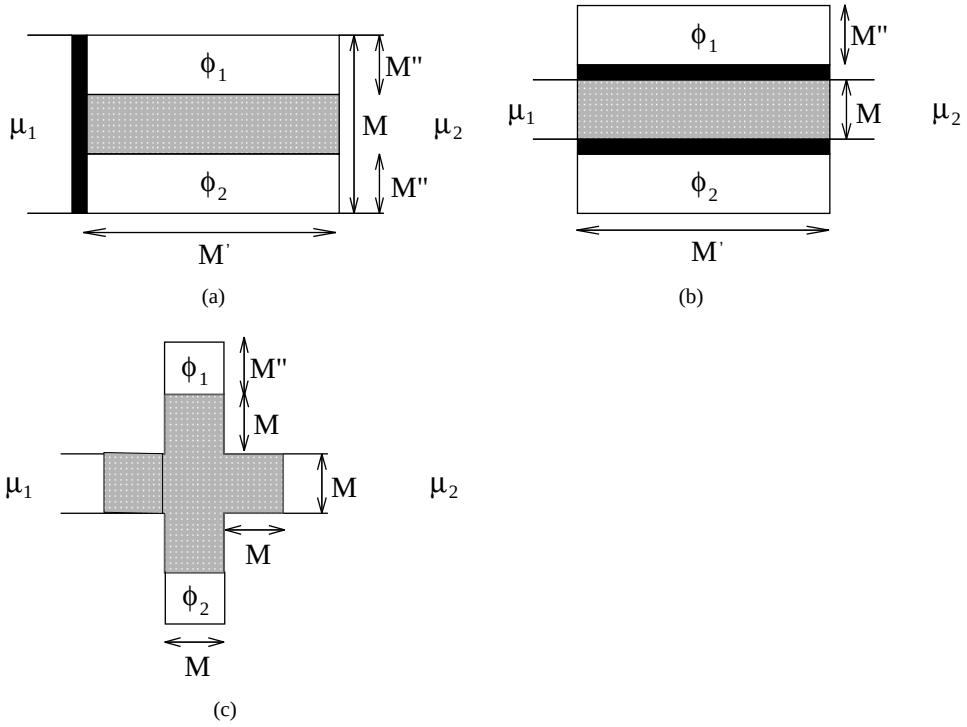

Figure 1. Three possible interferometers, each with two superconducting regions of width M''. In (a) and (b), the superconductors are separated by a distance M and in (c) by a distance $3M$. The scattering region is connected to normal, external current-carrying leads, of width $M + 2M''$ in (a), and of width M in (b) and (c). In (a) and (b), a normal barrier (shown black) is placed at the N–S interface. The current flows from left to right between external reservoirs with potentials μ_1 and μ_2. In the tight-binding model used in the numerical simulations, the barrier comprises a line of sites with diagonal elements $\epsilon_i = \epsilon_b$.

Figure 1 shows three examples of interferometers, for which results are presented below. Each has two superconducting regions with definite phases ϕ_1 and ϕ_2, in contact with a normal region (shown shaded). In each case the scattering region is connected to normal, external current-carrying leads, with N conducting channels. In figures 1(a) and 1(b), a normal barrier (shown black) is placed at the N–S interface. In what follows we first show numerical results obtained from a two-dimensional, tight-binding model on a square lattice, with diagonal elements ϵ_i and nearest-neighbour hopping elements of magnitude unity. In the external leads we choose $\epsilon_i = 0$, yielding a Fermi energy of $E_F = 4$, equal to half the band width. In the single line of sites forming the barrier, $\epsilon_i = \epsilon_b$, and in the superconductors, where the order parameter magnitude $|\Delta| \neq 0$, we choose $\epsilon_i = 0$. In a

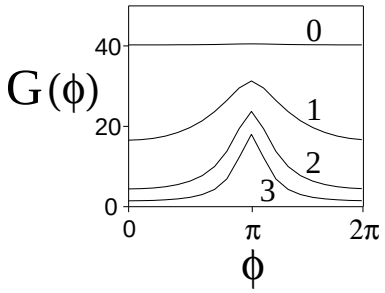

Figure 2. Numerical results for the conductance G of the structure of figure 1(a), with $M = 45, M' = 50, M'' = 15$, and number of open channels $N = 45$. Results are shown for $|\Delta = 0.1|$ and barrier potentials $\epsilon_b = 0, 1, 2, 3$. The number adjacent to a given curve is the corresponding value of ϵ_b.

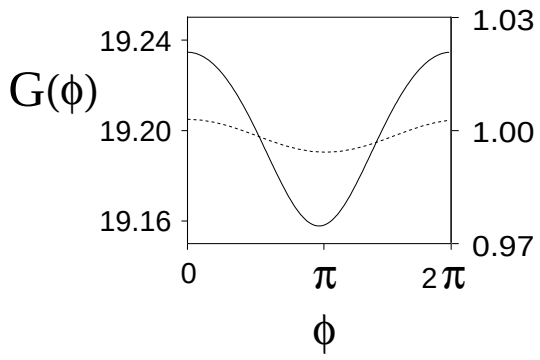

Figure 3. Results for the conductance G of the structure of figure 1(b) (solid line: left-hand scale) with $M = M' = M'' = 10, W = 0$, and that of figure 1(c) (dashed line: right-hand scale) with $M = M' = M'' = 10, W = 0$. $N = 10$ and $|\Delta| = 0.2$ in both cases. For the structure of figure 1(b) results are shown for a barrier potential $\epsilon_b = 2$.

disordered region of the sample, ϵ_i is chosen to be a random number uniformly distributed over the interval $\pm W$, whereas for a clean system, $W = 0$. As discussed in [16], the conductance is obtained by first evaluating the quantum mechanical scattering matrix and then evaluating the zero-temperature conductance formula (1). The transfer matrix codes used [16] are extremely versatile and can be used to analyse arbitrary geometries, with multiple contacts.

For the structure of figure 1(a), figure 2 shows numerical results for giant oscillations in the electrical conductance $G(\phi)$. In the absence of a barrier ($\epsilon_b = 0$), the amplitude of oscillation (in units of $2e^2/h$) is negligible compared with unity, whereas for $\epsilon_b = 1, 2, 3$ a large-amplitude oscillation is present. As the barrier strength ϵ_b increases, the amplitude of oscillation initially increases to a value of order Ne^2/h, before decreasing in proportion to the zero-phase conductance.

These results show that at intermediate barrier strengths, the relative amplitude as well as the absolute amplitude is optimized. Figure 3 shows results for the phase-periodic conductance of the structures of figure 1(b) (solid line) and figure 1(c) (dashed line). For the structure of figure 1(b) we have presented results in figure 3 for the most favourable barrier strength, in the absence of disorder. Introducing normal disorder or changing the barrier

strength decreases the amplitude of oscillation. In the case of the structure of figure 1(c) there is no barrier, but a disorder comparable to that in the experiments of reference [5] has been used. We have examined the structures in figures 1(b) and 1(c) for a variety of barrier strengths and disorders, respectively, and in no case have we found an amplitude which is more than a few per cent of $2e^2/h$.

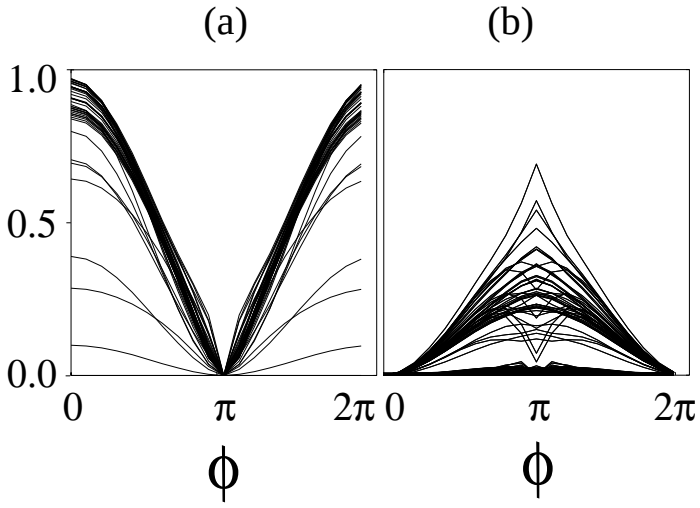

Figure 4. (a) Numerical results for the diagonal Andreev reflection coefficients $(R_a)_{ii}$ for the structure of figure 1(a), with $M = 45$, $M' = 50$, $M'' = 15$, $N = 45$, and no barrier present ($\epsilon_b = 0$). (b) Corresponding results for the off-diagonal coefficients $(R_a)_{ij}$ with $i \neq j$.

We now develop an analytic, multiple-scattering description of a clean N–S interface, which emphasizes the crucial role of normal scattering in optimizing this effect and which captures the essential physics of interferometers. Consider first an idealization of the structure of figure 1(a), in which the distance M between the superconductors vanishes and therefore for a long enough sample there is no quasi-particle transmission. In this limit the total resistance reduces to a sum of two measureable boundary resistances, and in what follows, we therefore focus attention on the left-hand boundary conductance [9, 17]:

$$G_{\mathrm{B}}(\phi) = 2R_a = 2\,\mathrm{Tr}\; r_a r_a^{\dagger} = \sum_{i,j=1}^{N} (R_a)_{ij} \tag{2}$$

where $(R_a)_{ij} = |(r_a)_{ij}|^2$ is the Andreev probability of reflection from channel j to channel i. As in equation (1), the Andreev reflection coefficient is of the form $R_a = R_{\mathrm{diag}} + R_{\mathrm{off-diag}}$ where $R_{\mathrm{diag}} = \sum_{i=1}^{N} (R_a)_{ii}$ and $R_{\mathrm{off-diag}}$ is the remaining contribution from inter-channel scattering, $R_{\mathrm{off-diag}} = \sum_{i \neq j=1}^{N} (R_a)_{ij}$.

In the absence of disorder, for $M = 0$ and $\phi = 0$, translational symmetry in the direction transverse to the current flow guarantees that $R_{\mathrm{off-diag}} = 0$. For the system of figure 1(a), with no barrier, no disorder and $M = 45$, figure 4(b) shows the behaviour of the coefficients $(R_a)_{ij}$ for $i \neq j$ and demonstrates that even for finite M, off-diagonal scattering at $\phi = 0$ is negligible. This figure leads us to a second observation, namely that even for non-zero ϕ, almost all of the off-diagonal coefficients are negligibly small, and that a given channel i couples strongly to at most one other channel j. Consequently in the absence of disorder, a multiple-scattering description involving pairs of channels captures the essential physics.

Consider a normal barrier to the left of a N–S interface. Particles (holes) impinging on the normal scatterer are described by a scattering matrix s_{pp} (s_{hh}), and those arriving at the N–S interface are described by a reflection matrix ρ, where

$$s_{pp} = \begin{pmatrix} r_{pp} & t'_{pp} \\ t_{pp} & r'_{pp} \end{pmatrix} \qquad \rho = \begin{pmatrix} \rho_{pp} & \rho_{ph} \\ \rho_{hp} & \rho_{hh} \end{pmatrix}.$$

The elements of s and ρ are themselves matrices describing scattering between open channels of the external leads. For an ideal interface, where Andreev's approximation is valid [1], ρ_{pp} and ρ_{hh} are negligible and in what follows will be set to zero. As a consequence, ρ_{hp} and ρ_{ph} are unitary and one obtains [18] $r_a = t'_{hh}\rho_{hp}M_{pp}^{-1}t_{pp}$, with $M_{pp} = 1 - r'_{pp}\rho_{ph}r'_{hh}\rho_{hp}$. In contrast with the analysis of [18], where ρ_{hp} is proportional to the unit matrix, the interference effect of interest here is contained in the fact that ρ_{hp} induces off-diagonal scattering. Substituting r_a into equation (2) and taking advantage of particle–hole symmetry at $E = 0$ yields

$$G = 2\,\mathrm{Tr}(T\,Q^{-1}T(Q^{\dagger})^{-1}) \tag{3}$$

where $Q = \rho^{\mathrm{t}}_{ph} + (r')_{pp}\rho_{ph}(r')^{\dagger}_{pp}$, with $T = t_{pp}t^{\dagger}_{pp}$ the transmission matrix of the normal-scattering region. This multiple-scattering formula for the boundary conductance is valid in the presence of an arbitrary number of channels and in any dimension. Notice that if T is equal to the unit matrix, then $Q = \rho^{\mathrm{t}}_{ph}$ and therefore $G = 2N$, irrespective of the phase-periodic nature of ρ_{ph}. This demonstrates that at a clean interface, whatever the phase, the approximate unitarity of ρ_{ph} yields the sum rule $R_{\mathrm{diag}} + R_{\mathrm{off-diag}} = N$ and therefore the conductance is independent of ϕ. More generally, whenever normal reflection (R_0) and Andreev transmission (T_a) are negligibly small, unitarity imposes the sum rule $T_0 + R_a = N$, and since in this limit equation (1) reduces to $G = T_0 + R_a$, the amplitude of oscillation must vanish.

Equation (3) is very general and makes no assumption about the nature of matrices ρ_{ph} and s_{pp}. We now introduce a two-channel model in which ρ_{ph} is chosen to be an arbitrary two-dimensional unitary matrix. In the absence of disorder, t_{pp} and r_{pp} are diagonal and therefore the only interchannel coupling is provided by ρ_{ph}. Substituting these matrices into equation (3) yields an expression for r_a involving a single phase θ, whose value is a linear combination of phase shifts due to normal reflection at the barrier, Andreev reflection at the N–S interface, and the phase accumulated by an excitation travelling from the barrier to the interface. The result for the sum of the diagonal elements is

$$R_{\mathrm{dia}}(\phi,\theta) = (R_a)_{11} + (R_a)_{22} = \frac{cA}{(cC + s(D - E\cos\theta))^2} \tag{4}$$

and for the sum of the off-diagonal elements

$$R_{\mathrm{off-diag}}(\phi,\theta) = (R_a)_{12} + (R_a)_{21} = \frac{sB(D - E\cos\theta)}{(cC + s(D - E\cos\theta))^2} \tag{5}$$

where $A = T_1^2(1+R_2)^2 + T_2^2(1+R_1)^2$, $B = 2T_1T_2$, $C = (1+R_1)(1+R_2)$, $D = 1 + R_1R_2$, $E = 2\sqrt{R_1R_2}$, $R_1 = 1 - T_1$, $R_2 = 1 - T_2$, $c = \cos^2\phi/2$, and $s = \sin^2\phi/2$. After averaging over the rapidly varying phase θ, this yields

$$R_{\mathrm{dia}}(\phi) = cA\frac{cC + sD}{((cC + sD)^2 - s^2E^2)^{3/2}} \qquad R_{\mathrm{off-diag}}(\phi) = sB\frac{cCD + s(D^2 - E^2)}{((cC + sD)^2 - s^2E^2)^{3/2}}. \tag{6}$$

For a given value of ϕ, once the normal-barrier-transmission coefficients T_1 and T_2 of the two channels are chosen, the right-hand sides of equations (6) are completely determined.

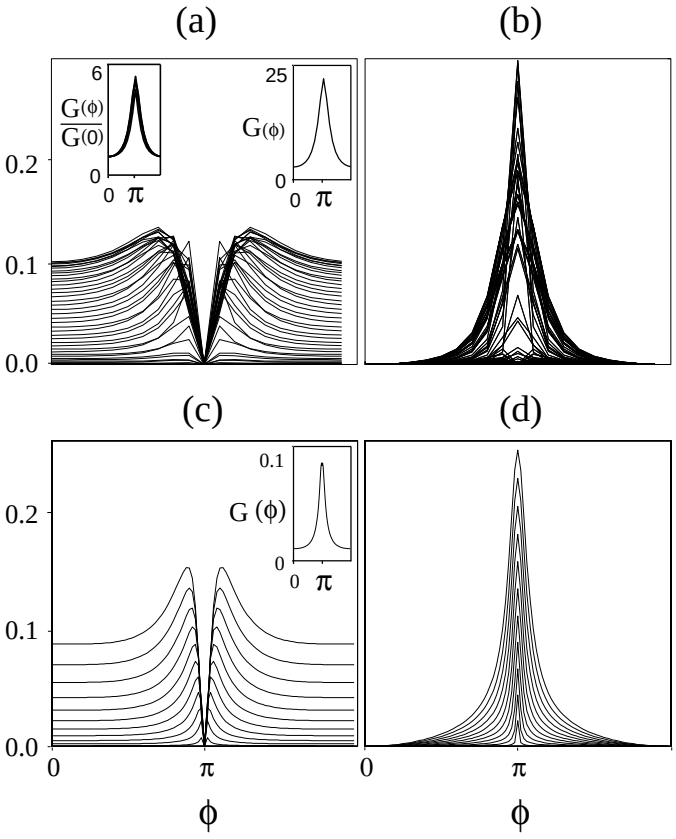

Figure 5. (a) Numerical results for the diagonal Andreev reflection coefficients $(R_a)_{ii}$ of the structure of figure 1(a), with $M = 45$, $M' = 50$, $M'' = 15$, $N = 45$, and barrier potential $\epsilon_b = 2$. (b) Corresponding results for the off-diagonal coefficients $(R_a)_{ij}$ with $i \neq j$. (c), (d) Analytical results from a two-channel calculation. The insets in the top right-hand corners of (a) and (c) show the corresponding conductances. The top left-hand inset of (a) shows plots of $G(\phi)/G(0)$ for the five values $N = 35, 40, 45, 50, 55, 60$.

In what follows, we compare analytic results for $R_{\rm dia}(\phi)$ and $R_{\rm off-diag}(\phi)$ with numerical results for $(R_a)_{ij}$. For the structure of figure 1(a), figures 4(a) and 4(b) show numerical results for the diagonal $(R_a)_{ii}$ and off-diagonal coefficients $(R_a)_{ij}$ $(i \neq j)$ respectively. Notice that at zero phase, most of the diagonal coefficients $(R_a)_{ii}$ are close to unity, although a small number of order $N|\Delta|/E_F$ are suppressed, due to a breakdown of Andreev's approximation for low-angle scattering [19]. This slight breakdown of Andreev's approximation yields a small-amplitude oscillation even in the absence of normal potential scattering, but as emphasized by figure 2, the fractional amplitude is negligible. Figures 5(a) and 5(b) show corresponding results for the diagonal and off-diagonal coefficients in the presence of a barrier. At $\phi = 0$, there is no coupling between the channels, and the scattering properties are those of N independent channels, each with a barrier transmission coefficient T_i. The spectrum of coefficients depends in detail on the shape of the barrier. The top right-hand inset of figure 5(a) shows the boundary conductance $G(\phi)$ obtained by summing the curves in figures 5(a) and 5(b), as well as the contribution due to normal transmission. Figures 5(c) and 5(d) show analytic results for $R_{\rm dia}(\phi)$ and $R_{\rm off-diag}(\phi)$

obtained from equations (6) and (7) by choosing ten pairs of transmission coefficients T_1, T_2, with $T_2 = 0.2T_1$. The inset of figure 5(c) shows the corresponding conductance obtained by summing the curves in figures 5(c) and 5(d).

Clearly the qualitative features of the exact simulation are reproduced by this two-channel analysis. Since the latter yields the N-channel conductance via a summing over $N/2$ independent pairs of channels, the amplitude of the oscillation is predicted to scale with the number of open channels. This is confirmed by the exact numerical results shown in the top left-hand inset of figure 5(a), which shows plots of $G(\phi)/G(0)$ for five values of N ranging from $N = 35$ to $N = 60$.

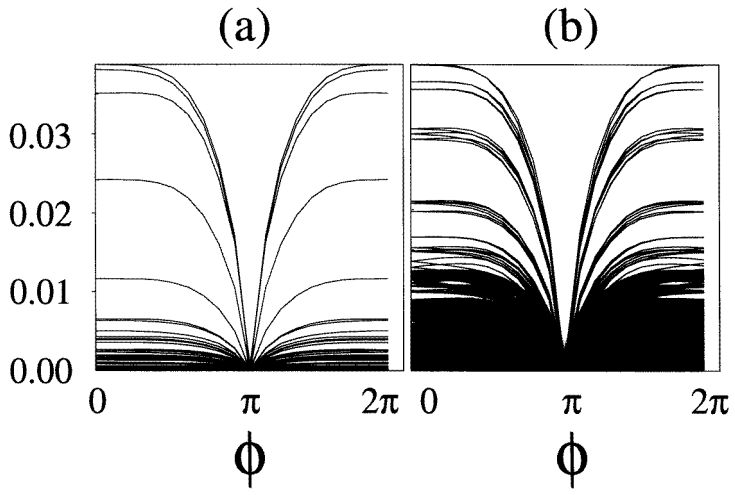

Figure 6. Numerical results obtained from a tight-binding model of the structure of figure 1(a), but with the barrier replaced by a disordered region of length 30 sites. In these simulations, $M = 45$, $M' = 15$, $M'' = 50$, $N = 45$, $\Delta_0 = 0.1$, and the disorder is $W = 2.8$. (a) and (b) show diagonal and off-diagonal Andreev reflection coefficients, respectively.

Analytically we find that at $\phi = 0$ and $\phi = \pi$, in the absence of disorder, the second derivative of the two-channel conductance satisfies $\mathrm{d}^2G/\mathrm{d}\phi^2 \geqslant 0$, for all barrier strengths. However, at $\phi = \pi$, as shown in the inset of figure 5(c), the conductance is close to maximal, with only a local, barely discernible minimum. The exact numerical results shown in the insets of figure 5(a) reveal a zero-phase minimum, and a careful examination around the peak value reveals a maximum at $\phi = \pi$. From figure 4, it is clear that the nature of the extrema is the result of competition between diagonal Andreev reflection coefficients, which exhibit a zero-phase maximum and off-diagonal coefficients which possess a zero-phase minimum. At $\phi = \pi$, the latter dominate and $G(\pi)$ is maximal. This contrasts with the predictions of [9, 11–13], which for a spatially symmetric structure, in the presence of disorder, yield $G(\pi) = 0$. To illustrate the qualitative changes occurring in the presence of disorder, figure 6 shows numerical results for the structure of figure 1(a), with $M = 45$, $M' = 50$, $M'' = 15$, but with the barrier replaced by a disordered normal square of width 30 sites. This shows that replacing the barrier by a disordered region causes the zero-phase extremum of the off-diagonal coefficients to switch from a minimum to a maximum. Since the total conductance is a sum of all curves in figure 6, $G(0)$ switches to a maximum and $G(\pi)$ to a minimum. On the one hand, channels no longer couple in pairs and therefore a complete multi-channel

scattering description is needed. On the other, off-diagonal and diagonal elements are no longer out of phase and therefore theories describing average properties of a single channel, such as the quasi-one-dimensional descriptions of [9, 11–13], become appropriate.

In summary, through exact solutions of the Bogoliubov–de Gennes equation, we have demonstrated that giant oscillations are obtainable and can be observed by breaking a crucial sum rule. It should be noted that the possibility of giant conductance oscillations in the ballistic regime has also been pointed out in [20], using a geometry different from that discussed here. The main differences are that in the geometry of [20], the phase difference is along the longitudinal direction, interchannel scattering is absent, and the sum rule is automatically broken by the presence of beam-splitters.

Remarkably, the structure of figure 1(c) shows only a small mesoscopic effect, with an amplitude much smaller than that observed in the experiments of [5]. In a recent publication [21] it was demonstrated that at finite voltages the amplitude of oscillation for this structure is significantly enhanced and therefore by reducing the temperature or measuring voltage in these experiments, we predict that the amplitude of oscillation will decrease. More crucially, in the presence of a normal barrier at the interface, we predict that the structure of figure 1(a) will be found to be more optimal, and that in metallic samples, with very large N, the amplitude of oscillation could become orders of magnitude larger than $2e^2/h$.

This work was supported by the EPSRC, the EC Human Capital and Mobility Programme, NATO, the MOD and the Institute for Scientific Interchange (Torino). It has benefited from useful conversations with V Petrashov, F Sols, and C W J Beenakker.

References

[1] Andreev A F 1964 *Sov. Phys.–JETP* **19** 1228
[2] Price J, private communication
[3] Pothier H, Gueron S, Esteve D and Devoret M H 1994 *Physica* B **203** 226
[4] van Wees B J, Dimoulas A, Heida J P, Klapwijk T M, van de Graaf W and Borghs G 1994 *Physica* B **203** 285
[5] Petrashov V T, Antonov V N, Delsing P and Claeson T 1995 *Phys. Rev. Lett.* **74** 5268
[6] de Vegvar P G N, Fulton T A, Mallison W H and Miller R E 1994 *Phys. Rev. Lett.* **73** 1416
[7] Spivak B Z and Khmel'nitskii D E 1982 *JETP Lett.* **35** 413
[8] Al'tshuler B L and Spivak B Z 1987 *Sov. Phys.–JETP* **65** 343
[9] Lambert C J 1991 *J. Phys.: Condens. Matter* **3** 6579
[10] Hui V C and Lambert C J 1993 *Europhys. Lett.* **23** 203
[11] Hekking F W J and Nazarov Yu V 1993 *Phys. Rev. Lett.* **71** 1625
[12] Nazarov Yu V 1994 *Phys. Rev. Lett.* **73** 1420
[13] Zaitsev A V 1994 *Phys. Lett.* **194A** 315
[14] Beenakker C W J, Melsen J A and Brouwer P W 1995 *Phys. Rev.* B **51** 13 883
[15] van Wees B J, Dimoulas A, Heida J P, Klapwijk T M, van de Graaf W and Borghs G 1994 *Physica* B **203** 285
Dimoulas A, Heida J P, van Wees B J and Klapwijk T M 1995 *Phys. Rev. Lett.* **74** 602
[16] Lambert C J, Hui V C and Robinson S J 1993 *J. Phys.: Condens. Matter* **5** 4187
[17] Blonder G E, Tinkham M and Klapwijk T M 1982 *Phys. Rev.* B **25** 4515
[18] Beenakker C W J 1992 *Phys. Rev.* B **46** 12 841
[19] Claughton N R, Hui V C and Lambert C J 1995 *Phys. Rev.* B **51** 11 635
[20] Kadigrobov A, Zagoskin A, Shekhter R and Jonson M 1995 *Phys. Rev.* B **52** R8662
[21] Volkov A, Allsopp N K and Lambert C J 1996 *J. Phys.: Condens. Matter* **8** L45